A unified crowd simulation model revealing relationships among "Physiology-Psychology-Physics" factors

Mingliang Xu, Chaochao Li, Pei Lv, Wei Chen, Zhigang Deng, Bing Zhou and Dinesh Manocha

Abstract—We present a unified model for crowd simulation, CubeP, which comprehensively considers physiological, psychological, and physical factors. Inspired by the theory of "the devoted actor," the movements of each individual in our model are determined by modeling the physical influence of physical strength consumption and the emotion of panic. In particular, human physical strength consumption is computed using a physics-based numerical method. Inspired by the James-Lange theory, panic emotion is estimated by means of an enhanced emotional contagion model that leverages the inherent relation between physical strength consumption and panic emotion. To the best of our knowledge, our model is the first method that integrates physiological, psychological, and physical factors together and exploits the relationship between these factors. We highlight the performance on different scenarios and compare the resulting behavior with real-world video sequences. Our approach can reliably predict the changes in physical strength consumption and panic emotion of individuals in an emergency situation.

Index Terms—Crowd simulation, emotional contagion, physical strength, James-Lange theory

1 INTRODUCTION

EFFICIENT and accurate crowd simulation is one of the most important research topics in the field of computer graphics and public safety [1]. There are no known computational models that can simulate realistic crowd behaviors in all kind of situations and take into account various complex factors. At a broad level, crowd behavior is governed by psychological and physiological factors [2].

The main purpose of crowd simulation algorithms is to model the movements of individuals in a crowd realistically [3], which includes three aspects: physical, physiological, and psychological factors. The individual movement (in terms of speed and direction), physical strength consumption, and panic emotion [4] are the physical, physiological, and psychological factors, respectively. These three factors influence one another and evolve dynamically. It is important to describe the inherent relationship among these three factors, which is more obvious in emergency or evacuation situations [5]. Most previous methods only consider the physiological or psychological factors but have not tried to combine them with other issues that govern behavior or movement [6]. Some crowd simulation algorithms take into account the physical strength [7]. Physical strength is a person's or animal's ability to exert force on physical objects using muscles [8]. Physical strength consumption is defined as the energy expenditure [9] of a human which directly affects the moving speed of an individual [10]. Moreover, some approaches incorporate the panic emotions of individuals in crowd simulations, which is one of the most commonly used psychological factors [11]. Panic emotion can hinder an individual to take proper actions in emergency situations [4]. Researchers have observed that the occurrence of danger can directly cause the changes of panic emotion in an individual, thereby further determining his or her movements [12]. We mainly focus on panic emotion in emergency situations. However, it is difficult to describe the inherent relationship between physical strength consumption and panic emotion and then combining these factors to determine the movement of each individual [5]. Therefore, incorporating them into a unified model for crowd simulation is challenging, as we describe below:

(1) It is difficult to model the physical strength consumption of an individual in a crowd accurately [13]. This task involves considering many factors that are needed to quantify the influence of physical strength consumption on crowd movement [7].

(2) Modeling the individual panic emotion in a crowd accurately is difficult because of its constant and dynamic changes [14]. Various factors, such as physical strength consumption and individual movement, affect panic emotions.

Inspired by the theory of "the devoted actor" [2], which shows that both psychological and physiological states have effects on an individual's physical state, we propose the first (to the best of our knowledge) unified model that combines the physiological, psychological, and physical factors to address these challenges (illustrated in Figure 1). The main contribution of this paper is that we present the relationship among these three factors in emergency or evacuation

- *Mingliang Xu, Chaochao Li, Pei Lv, and Bing Zhou are with Center for Interdisciplinary Information Science Research, ZhengZhou University, 450000.*
- *Wei Chen is with State Key Lab of CAD&CG, Zhejiang University, 310058.*
- *Zhigang Deng is with Department of Computer Science, University of Houston, Houston, TX, 77204-3010.*
- *Dinesh Manocha is with Department of Computer Science and Electrical & Computer Engineering, University of Maryland, College Park, MD, USA.*
  E-mail: {iexumingliang, ielvpei, iebzhou} @zzu.edu.cn; zzulcc@gs.zzu.edu.cn; chenwei@cad.zju.edu.cn; zdeng4@uh.edu; dm@cs.umd.edu

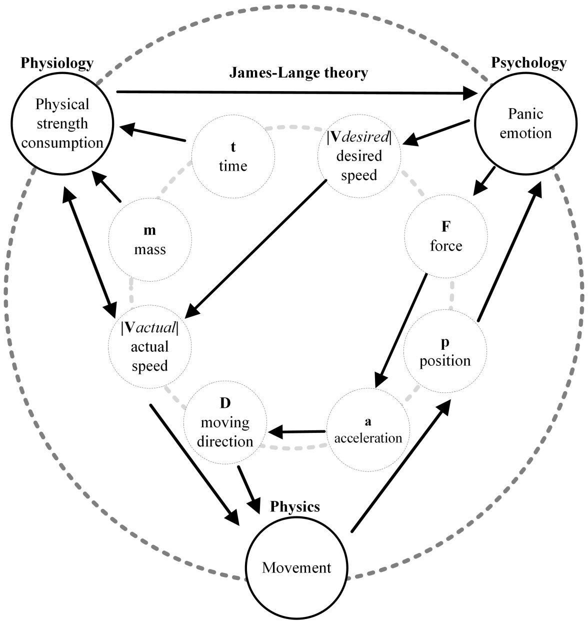

Fig. 1: The relationships among the physiological (physical strength consumption), psychological (panic emotion), and physical (movement) factors of moving individuals in a crowd. Physical strength consumption is calculated according to the actual speed, mass, and moving time of individuals. The panic emotion is determined by the position and physical strength consumption of the individual, and it will further affect the individual's desired speed. Moreover, one's current panic emotion will affect each individual's moving direction by changing its acceleration based on the inferred force. These three factors affect one another and we highlight their combined effect on the crowd's movement.

situations. These relationships are summarized as follows:

- We introduce a physical strength consumption calculation method based on how individuals work based on the laws of physics [15] and quantitively characterize the dynamic changes of the calculation. We also present the relationship between physical strength consumption and moving speed.
- We improve the traditional emotional contagion model [11] based on the James-Lange theory [5]. Our new proposed model not only analyzes emotional contagion, but also depicts the relationship between physical strength consumption and panic emotion and how panic emotion determines the movement.

The rest of this paper is organized as follows. Background and related work are reviewed in Section 2. The definition of our proposed crowd simulation model is introduced in Section 3. Experiments are presented in Section 4.

2 Related Work

In this section, we provide a brief overview of prior work on crowd simulation, dividing the summaries based on whether the works involve physical, psychological, or physiological factors.

2.1 Traditional crowd simulation models

We summarize representative crowd simulation models in this subsection without considering psychological or physiological factors [16], [17], [18].

In the real world, many environmental factors influence individual movement, i.e. scene layout, moving pedestrians, and stationary groups [19], [20]. During the evacuation of a crowd, the behavioral choice of an individual is highly dependent on the moving directions of nearby individuals, the hazard location, and obstacles [21]. Cassol et al. [22] focus on global path planning and their main goal is to identify the best evacuation routes for a specific population, when leaving a certain building. To realize better behavioral choices, most approaches calculate the position of each individual at the next time step to obtain a conflict-free moving path in a global scenario [23]. However, these approaches are not applicable to highly complex scenes with dense crowds since they have many restrictive conditions around different obstacles. Other approaches use local obstacle avoidance methods. Namely, once the movement state of an individual is determined, the movement states of other individuals are updated by iterating the premise of collision avoidance [24].

Unfortunately, these approaches still face difficulties in accurately controlling individual movements. Researchers in this field are increasingly focusing on integrating global path planning and local obstacle avoidance [25]. Weiss et al. [26] model collision avoidance constraints both in short ranges and long ranges to deal with sparse and dense crowds. In [27], intergroup- and intragroup-level techniques are presented to perform coherent and collision-free navigation using reciprocal collision avoidance. Mutual information about the dynamic crowd is used to guide agents' movements by combining both macroscopic and microscopic controls [28]. By constructing a visual tree, the shortest path without collision is obtained in [29]. In addition, in [30], [31], [32], and [33], path planning and navigation algorithms are described for crowd simulation in complex contexts. Furthermore, in [34], an effective long-range collision avoidance algorithm is proposed.

In contrast to these works, our model enhances the traditional social force model to avoid collisions with surrounding individuals and obstacles by combining panic emotion and physical strength consumption calculations. Traditional crowd simulation models are not concerned with this approach. In our model, we mainly deal with the moving directions and moving speeds which are largely influenced by the panic emotion and physical strength consumption during a relatively short period of time.

2.2 Crowd simulation with psychological factors

The psychological state of an individual plays a vital role in his or her decision-making process [35], [36], [37]. Stress and panic emotion are typical psychological factors and have a great influence on the movement of individuals in a crowd. In this subsection, we introduce representative works on them.

In [14], authors focus on stress, which is defined as any change caused by interactions between the environment and individuals. Generally, stress is caused by a discrepancy between environmental demands and the abilities of individuals. Stress can have positive effects on individual behavior. In emergency or evacuation situations, stress improves the performance of individuals [14]. It can be chronic and long-term [14]. However, stress and panic emotion are inherently different. Panic emotion is short-term and changeable [38] and usually leads to a negative effect on individuals [39]. One of the most disastrous forms of collective human behavior is the kind of crowd stampede induced by panic emotion, often leading to fatalities as people are crushed or trampled [12].

Stress and panic emotion of individuals are mirrored by others and they are disseminated within the crowd [11]. There are two separate lines of emotional contagion research: epidemiological-based and thermodynamics-based.

The epidemiological SIR model [40] divides the individuals in a crowd into three categories: infected, susceptible, and recovered. The spread of disease among these three groups is analyzed. This model has also been extended to other different fields. In [41], the extended model is used to simulate the spread of rumor. Some researchers use the epidemiological SIR model in conjunction with other models to describe emotion propagation under specific situations. The cellular automata model is used to simulate the spread of infectious diseases in [42]. In [11], the epidemiological SIR model is improved through its combination with the OCEAN model [43]. The phenomenon of emotional contagion occurs more obviously in a panicked crowd. In [44], a qualitatively simulated approach to modelling emotional contagion is proposed for a large-scale emergency evacuation. This approach confirms that the effectiveness of rescue guidance is influenced by the leading emotion in the crowd. Moreover, in [45] the cellular automata model based on the SIR model (CA-SIRS) is used to describe emotional contagion in the crowd-moving process during an emergency situation.

A thermodynamics-based emotion contagion model was introduced by Bosse et al. [46] in the ASCRIBE system. The authors use a multi-agent-based approach to define emotion contagion within groups. Their study focuses on emotions as a collective entity rather than the emotions of single individuals. Neto et al. [36] adapt the model of Bosse et al. [46] into BioCrowds and cope with different groups of agents. In [47], dynamic emotion propagation is described from the perspective of social psychology with a combination of thermodynamic-based models and epidemiological-based models.

Because panic emotion has a great influence on individual movement and often lead to serious consequences, we focus on panic emotion in emergency situations. Inspired by the James-Lange theory in biological psychology, we improve the Durupinar model [11] by considering the influence of physical strength consumption on panic emotion. In contrast to previous methods considering only panic emotion, we further demonstrate the relationship between physical strength consumption and panic emotion.

2.3 Crowd simulation with physiological factors

To complete a comprehensive analysis of crowd movement, we must consider not only psychological factors, but also physiological factors of individuals because these factors are also very important in determining the crowd movement [10].

Physical strength is one of the most important physiological parameters that affects individual movement. Bruneau et al. [48] apply the principle of minimum energy (PME) on groups of different sizes and densities. In [9], [49], some physiological indicators (such as physical strength consumption and heart rate) are described. Furthermore, the relationship between physical strength consumption and heart rate is revealed, which is also a method for predicting physical strength consumption based on the heart rate during moderate and vigorous exercise. Work in [10] shows that the relationship between physical strength consumption and speed is nonlinear. In [7], researchers investigate how the cumulative consumption of physical strength affects the evacuation time of individuals. Guy et al. [15] propose the principle of least effort (PLE) to compute the physical strength consumption required by various movements. Furthermore, Guy et al. [50] propose a less energy-consuming, conflict-free crowd movement method based on the criterion of minimal physical strength consumption [15]. These approaches are focused on the relationship between physical strength and other physiological parameters (heart rate and oxygen uptake, for example) or individual movement. In [13], the authors choose other four basic physiological characteristics, including gender, age, health, and body shape, and map them to a navigation method.

Inspired by prior approaches, we focus on physical strength consumption, which is a very important physiological factor. Physical strength consumption is central to research in human biology and biological anthropology [51] and is closely related to a variety of factors such as heart rate, oxygen consumption, etc. [49]. It directly affects the moving speed of an individual [7]. Other physiological factors (such as gender, age, health, and body shape) can influence movement through physical strength consumption. we also describe the effect of physical strength consumption on the physical movements of individuals. Moreover, we analyze the relationship between physical strength consumption and panic emotion by emphasizing the interaction of individual physiological, psychological, and physical states.

3 CubeP-Crowds Model

The crowd simulation model proposed is named CubeP-Crowds Model (CubeP for short), and it comprehensively considers the physiological, psychological, and physical factors that influence crowd movement in a unified manner. The flowchart of the CubeP model is presented in Figure 2. Strenuous movements are often observed in individuals in emergency or evacuation situations, and the relationship among these factors is more obvious in such situations. Therefore, we mainly focus on simulating crowd movements in such emergency situations.

The CubeP model consists of three important components: physical strength consumption, panic emotion, and individual movement. Human physical strength consumption is computed with a physics-based method (Section 3.2). The panic emotion is determined through an enhanced emotional contagion model that leverages the inherent

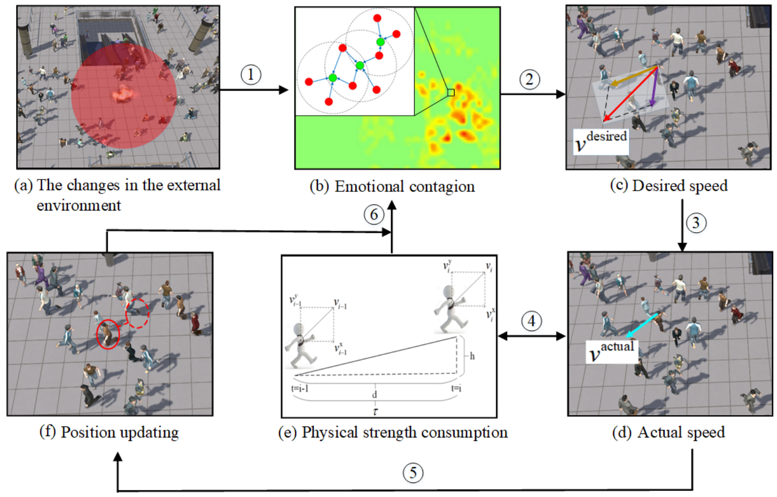

Fig. 2: The flowchart of the CubeP model. (a) Changes in the external environment can cause emotional fluctuations. For example, a hazard occurs and the red area represents the range of influence of the hazard. (b) The emotional changes of one individual are calculated according to the direct impact of the hazard and emotional contagion of his or her neighbors (Section 3.3). (c) The desired speed and direction of each individual are calculated based on an updated panic emotion (Section 3.4). (d) Due to the limit of physical strength consumption, the actual speed is further determined [10] (Section 3.4). (e) The calculation of physical strength consumption affected by the actual speed (Section 3.2). In contrast, the cumulative physical strength consumption also determines the actual maximal speed of the individual at the next time step (Section 3.4). The current physical strength consumption reflects the emotional experience of an individual (Section 3.3). (f) The position of the individual is updated according to its actual speed. If the individual is panicked, we return to step (b); otherwise, the flowchart ends (Section 3.3).

relationship between physical strength consumption and panic emotion (Section 3.3). The CubeP model computes the movement of an individual by modeling the physical influence of the physical strength consumption and the panic emotion (Section 3.4).

3.1 Symbols and Notations

For convenience, the important parameters and their descriptions used in the CubeP model are listed in Table 1.

3.2 Physical strength consumption calculation

Physical strength consumption is one of the most commonly used physiological indicators and closely related to individual movement. It is defined in the following equation:

$$P(t) = P_{hor}(t) + P_{ver}(t) \tag{1}$$

where $P(t)$ denotes the total physical strength consumption at time t and $P_{hor}(t)$, $P_{ver}(t)$ denote the physical strength consumption along the horizontal and the vertical directions, respectively. They are defined as follows:

$$P_{hor}(t) = \sum_{i=1}^{t} F_i^x \cdot d_i \tag{2}$$

$$P_{ver}(t) = \sum_{i=1}^{t} F_i^y \cdot h_i \tag{3}$$

F_i^x is the driving force of the individual along the horizontal direction. This force overcomes friction. d_i is the moving distance of the individual at time t. $F_i^x \cdot d_i$ represents the

TABLE 1: The parameters used in the CubeP model.

Notation	Description
$P(t)$	Physical strength consumption at time t
$P_{hor}(t)$	Physical strength consumption along the horizontal direction at time t
$P_{ver}(t)$	Physical strength consumption along the vertical direction at time t
F^x	Driving force of individual along the horizontal direction
F^y	Pulling force of individual along the vertical direction
E	Panic emotion
E_o	Emotional cognitive component
E_p	Emotional experience component
E_o^h	The emotion is effected from hazard.
E_o^c	Emotional contagion
EE	Energy expenditure
$V_i(t)$	Moving direction of the individual i at time t
$V_i^s(P,t)$	Safety evacuation direction of the individual i at position P and at time t
$V_i^{round}(t)$	Combined moving directions of individuals who are in the perceived range of the individual i at time t
$v_i^{desired}$	The desired speed $v_i^{desired}$ of the individual i considers only the emotion factor.
v_i^{actual}	The actual speed v_i^{actual} of the individual i is limited by his own physical strength consumption.
v^p	Maximum speed v^p according to current physical strength consumption
v_i^{MAX}	Maximum speed that the individual i can run
v_i^{NOR}	Speed of the individual i in the normal case (emotion value is equal to zero)

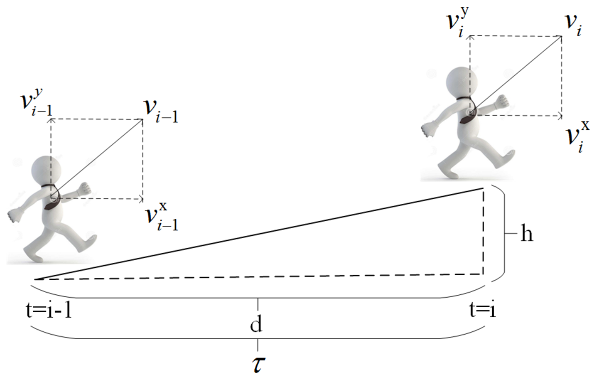

Fig. 3: Schematic of the physical strength consumption calculation. v_i^x is the velocity component of an individual in the horizontal direction at time i, and the length of each time step is τ. The horizontal speed of the individual changes from v_{i-1}^x to v_i^x in time interval τ.

work done by the individual along the horizontal direction. F_i^y is the pulling force of the individual along the vertical direction. This force overcomes gravity. h_i is the rising height of the individual at time t, and $F_i^y \cdot h_i$ represents the work done by the individual along the vertical direction.

According to the laws of physics, F_i^x is defined as follows:

$$F_i^x = f_i + \frac{(v_i^x - v_{i-1}^x)m}{\tau} \tag{4}$$

A diagram of the physical strength consumption calculation is shown in Figure 3.

The friction f_i is defined in Equation 5, k_i is defined in Equation 6, and t_i is defined in Equation 7 according to [52], [53]. μ is the friction factor, which is related to the shoes and the ground. In our implementation, μ=0.58 is adopted, which is also recommended in [54]. v_i is the current velocity magnitude, v_{min} is the minimal velocity magnitude, and v_{max} is the maximal velocity magnitude.

$$f_i = t_i \cdot \mu \cdot mg \cdot k_i \tag{5}$$

$$k_i = 1.5 + 0.5 \cdot \frac{v_i - v_{min}}{v_{max} - v_{min}} \tag{6}$$

$$t_i = 0.6 - 0.2 \cdot \frac{v_i - v_{min}}{v_{max} - v_{min}} \tag{7}$$

where k_i is the coefficient of the weight, t_i is the time of the individual's foot touching the ground, $k_i \propto v_i$, $t_i \propto^{-1} v_i$, $f_i \propto k_i$, and $f_i \propto t_i$. If one stands with both feet on a force plate, $t_i = k_i = 1$.

The physical strength consumption in the horizontal direction is defined by:

$$P_{hor}(t) = \frac{1}{2} \cdot \sum_{i=1}^{t} \left\{ \left((v_i^x)^2 - (v_{i-1}^x)^2 \right) m + t_i \cdot \mu \cdot mg \cdot k_i \left(v_i^x + v_{i-1}^x \right) \tau \right\} \tag{8}$$

According to the laws of physics, F_i^y is defined by the following equation:

$$F_i^y = mg + \frac{(v_i^y - v_{i-1}^y)m}{\tau} \tag{9}$$

where v_i^y is the velocity component in the vertical direction at time i.

The physical strength consumption in the vertical direction is defined by:

$$P_{ver}(t) = \frac{1}{2} \cdot \sum_{i=1}^{t} \left\{ \left((v_i^y)^2 - (v_{i-1}^y)^2 \right) m + \left(v_i^y + v_{i-1}^y \right) mg\tau \right\} \tag{10}$$

3.3 Panic emotion calculation affected by physical strength consumption

This section presents the calculation method for the panic emotion of an individual. The panic emotion $E \in [0,1]$, which indicates the level of panic approximatively. The panic emotion E consists of two components. The first is the emotional cognitive component E_o, which relates to the hazard and encompasses emotional contagion. The second is the emotional experience component E_p, which is calculated using physical strength consumption and heart rate. Therefore, the final emotion value is defined as follows:

$$E = w \cdot E_o + (1 - w) \cdot E_p \tag{11}$$

where w is a weighting parameter, and $0 < w < 1$.

3.3.1 *The emotional cognitive component*

In this section, we present the calculation method of E_o. E_o consists of three terms: effect from hazard E_o^h, emotional contagion E_o^c, and emotional attenuation E_o^d.

Effect from hazard $\boldsymbol{E_o^h}$: When individuals are able to perceive a hazard, they may become panicked. E_o^h is defined as follows:

$$E_o^h(P,t) = \sum_{s=0}^{n-1} \Gamma_s(P,t) \tag{12}$$

$$\Gamma_s(P,t) = \begin{cases} \frac{\alpha}{\sqrt{2\pi} \cdot r_s} e^{-\frac{(P-P_s)^2}{2{r_s}^2}} & \text{if } \| P - p_s \| < r_s \; and \; t \in U \\ 0 & \text{otherwise} \end{cases} \tag{13}$$

where P is the position of an individual, P_s is the position of a hazard, r_s is the radius of the influence range of the hazard, U is the duration of the hazard, and $\alpha (\alpha > 0)$ represents the strength of the hazard.

Effect from emotional contagion $\boldsymbol{E_o^c}$: There are two kinds of representative models of emotional contagion: the Neto model [36] and the Durupinar model [11]. They use fundamentally different mechanisms, but both can generate good results. However, the Neto model defines too many parameters for each pairwise interaction [55] and it is hard to compute these parameters automatically. Moreover, personality is also a very important, long-term, stable psychological factor and it is important for simulating heterogeneous crowd behavior [11]. The Neto model simplifies the personality factor while the Durupinar model pays more attention to that factor and is effective at capturing the differences between individuals. Personality is an important part of our CubeP model. We consider the effect of personality on panic emotion. According to this analysis, the Durupinar model is more suitable for the CubeP model. In the Virtual scenario of Section 4.2, we implement a comparable experiment to verify our motivation. Next, we present the emotional contagion method in the CubeP model.

During evacuation, individuals can be in one of two states: susceptible or infected. When the panic emotion of an individual exceeds a certain threshold T_1, the individual will be infected. If the panic emotion intensity of an individual surpasses another threshold T_2, then the individual can spread the panic emotion to his or her neighbors. In a general case, $T_1 < T_2$. T_1 and T_2 are correlated with individual personalities. Here we represent the personalities of individuals using the "OCEAN" personality model [11]. The personality of an individual is represented by a five-dimensional vector $< O, C, E, A, N >$. Each factor is randomly distributed with a Gaussian distribution $N(0, 0.25)$ [11]. $T_1 \propto^{-1}$ N, $T_1 \propto$ C [43]. $T_2 \propto^{-1}$ E [11], [43]. T_1 and T_2 are defined by the following:

$$T_1 = \alpha \cdot C - \beta \cdot N + \gamma \tag{14}$$

where $\alpha = 0.1$, $\beta = 0.1$, and $\gamma = 0.15$.

$$T_2 = \delta - \xi \cdot E \tag{15}$$

where $\delta = 0.35$, and $\xi = 0.1$. These parameters are determined according to the methods in [56], [57].

Within the perceived range, when a susceptible individual i sees an expressive individual j (the panic emotion value is higher than threshold T_2), i gets exposed by receiving a random dose d_i from a specified probability distribution multiplied by the panic emotion intensity of j. The dose values are randomly distributed with a Gaussian distribution $N(0.3, 0.01)$. We denote the panic emotion value of individual j at the time t' as $e_j(t')$. The panic emotion value of individual i due to emotional contagion is defined in Equation 16.

$$E_{i,o}^{c}(P,t) = \sum_{t'=0}^{t} \sum_{\forall j | j \in \mathit{Visibility}(i) \wedge j \text{ is expressive}} d_i(t') e_j(t') \tag{16}$$

Effect from emotional attenuation E_o^d : Emotional attenuation is defined in Equation 17.

$$E_o^d(P,t) = E_o(P^{pre}, t-1) \cdot \eta_t \tag{17}$$

where $E_o^d(P,t)$ is an emotion decay function and η_t is the decay rate. η_t is positively related to the individual personality factor N , and it is defined as follows:

$$\eta(t) = \begin{cases} 0 & t < t_1 \\ \frac{e^{\beta_2(t-t_2)} - e^{\beta_2(t-1-t_2)}}{1+e^{\beta_2(t-t_2)}} + \alpha \cdot N & t \geq t_1 \end{cases} \tag{18}$$

where $\beta_2 > 0$, $\eta \propto N$, and $\alpha = 0.1$.

The change of emotional cognitive component $\Delta E_o(P,t)$ is defined in Equation 19. The E_o is defined in Equation 20.

$$\Delta E_o(P,t) = E_o^h(P,t) + E_o^c(P,t) - E_o^d(P,t) \tag{19}$$

$$E_o(P,t) = E_o(P^{pre}, t-1) + \Delta E_o(P,t) \tag{20}$$

3.3.2 *The emotional experience component*

In this section, we present the calculation method of E_p. Individual emotions undergo three stages: cognition, action, and experience. First, a event occurs, and the individual perceives the current scene (emotional cognitive stage). Subsequently, the individual acts in a way that corresponds with physiological changes (action stage). Finally, the individual has the emotional experience (experience stage) [5].

Under emergency situations, once a hazard occurs, the individuals around it immediately take different actions. This will require the physical strength consumption. The energy expenditure (physical strength consumption in a minute) is chosen as the measure of physiological changes. The current heart rate is calculated using the energy expenditure. Then, the increment of the emotional experience value is calculated based on the heart rate increment. Thereafter, the current emotional experience value E_p is obtained. The details of the calculation method are as follows.

Equation 21 describes the relationship between energy expenditure (KJ/min) and heart rate (beat/min) when individuals experience panic and attempt to escape from the hazard [49]. According to Equation 21, we can calculate the current heart rate (*HR*) based on *EE*.

$$\begin{aligned} \mathit{EE} = {} & \mathit{gender} \times (-55.0969 + 0.6309 \times \mathit{HR} + 0.1988 \times \mathit{weight} + \\ & 0.2017 \times \mathit{age}) + (1 - \mathit{gender}) \times (-20.4022 + 0.4472 \times \mathit{HR} - \\ & 0.1263 \times \mathit{weight} + 0.074 \times \mathit{age}) \end{aligned} \tag{21}$$

where gender=1 for males and 0 for females, age (year) $\in$ [19,45], and weight (kg) $\in$ [47,116].

Furthermore, according to [58], heart rate (HR) and intensity of anxiety or fear (emotional experience) are positively correlated. In [58], the heart rate per minute is recorded before and after an electric shock, and emotional experience is reported once per minute. $\triangle E_p$ and $\triangle HR$ are the increments of emotional experience and heart rate compared with the values when individuals are not panicked.

Using a linear curve fitting method, we can obtain the relationship between $\triangle HR$ and $\triangle E_p$.

$$\triangle E_p = 0.03669 \cdot \triangle HR - 0.0724 \tag{22}$$

E_p is defined in Equation 23 and $E_p(0) = 0$.

$$E_p(t) = E_p(t-1) + \Delta E_p(t) \tag{23}$$

3.4 Individual movement model

Based on the results of physical strength consumption and panic emotion, the movement of each individual can be determined accurately through two aspects: moving direction and moving speed.

3.4.1 *Moving direction*

When a hazard occurs, individuals who can perceive the hazard directly will be panicked and calculate their own safety evacuation directions $V_i^s(P,t)$. $V_i^{round}(t)$ is the combined moving directions of individuals who are in the perceived range of the individual i.

$$\vec{V_i^s}(P,t) = \begin{cases} \sum_{s=0}^{n-1} \Gamma_s(P,t) \cdot \vec{P_s P} & \text{if} \| P - P_s \| < r_s \text{ and } t \in U \\ \vec{V} & \text{otherwise} \end{cases} \tag{24}$$

$$V_i^{round}(t) = \sum_{\forall j | j \in \mathit{Visibility}(i) \wedge j \text{ is expressive}} V_j(t) \tag{25}$$

Finally, the moving direction $V_i(t)$ of actual velocity of an individual who directly perceives the hazard is defined as follows:

$$V_i(t) = E \cdot V_i^s(P,t) + (1 - E) \cdot V_i^{round}(t) \tag{26}$$

TABLE 2: Dependence of speed decay rate and maximal-limit speed on physical strength consumption. As the physical strength consumption increases, the maximal-limit speed decreases.

Physical strength consumption p **(J)**	**Decay rate** ξ $(\%)$	**Maximal-limit speed** v^p (m/s)
0.0000 – 20154.0000	100.0000	v_i^{MAX}
20154.0000 – 40279.6713	99.8500	$v_i^{MAX} \cdot 0.9985$
40279.6713 – 81121.0042	89.4200	$v_i^{MAX} \cdot 0.8942$
81121.0042 – 166258.8920	75.8000	$v_i^{MAX} \cdot 0.7580$
166258.8920 – 181569.6090	69.8200	$v_i^{MAX} \cdot 0.6982$
181569.6090 – 196355.1760	65.7200	$v_i^{MAX} \cdot 0.6572$

where E is the panic emotion value. The moving direction of an individual i is influenced by panic emotion, safety evacuation direction, and other neighboring panicked individuals.

Individual i can perceive the hazard indirectly through the surrounding panicked individuals. The individual i moves in the direction of $V_i(t)$, as shown in Equation 27. $V_i^{old}(t)$ is the moving direction of the individual i at the last moment when he is not panicked. The more panicked the individual is, the more easily he moves with other neighboring panicked individuals. Nonetheless, if the individual i is not panicked, he or she still moves in his or her original direction.

$$V_i(t) = (1 - E) \cdot V_i^{old}(t) + E \cdot V_i^{round}(t) \tag{27}$$

3.4.2 *Moving speed*

In a panic situation, the speed of an individual i is expressed by the following equation [12]:

$$v_i^{desired} = (1 - E) \cdot v_i^{NOR} + E \cdot v_i^{MAX} \tag{28}$$

where $v_i^{desired}$ is the speed considering only the emotion factor, and $0 \leq E \leq 1$. The speed of an individual in the normal case (the panic emotion value is equal to zero) is v_i^{NOR} , and the maximal speed is v_i^{MAX}. The more panicked an individual is, the faster his or her speed.

However, an individual is limited by his or her own physical strength consumption. In some cases, the moving speed of an individual cannot reach the desired speed due to the maximum limit dictated by current physical strength consumption. The actual speed cannot exceed the maximal speed v^p.

$$v_i^{actual} = min\left(v_i^{desired}, v^p\right) \tag{29}$$

The dependence of the decay rate and maximal speed on physical strength consumption is presented in Table 2.

The actual speed can be calculated using Equation 30.

$$v_i^{actual} = min\left((1 - E) \cdot v_i^{NOR} + E \cdot v_i^{MAX}, v_i^{MAX} \cdot \xi\right) \tag{30}$$

4 EXPERIMENTS

Our proposed algorithm is used to simulate crowd movement in various scenarios and we demonstrate the benefits of it in these different scenarios. The simulation results show that our proposed method can generate realistic group behavior. It can also reliably predict the changes of physical strength consumption and panic emotion of a crowd in an emergency.

(a) Positions of the individuals at the 10^{th} frame when the hazard occurs

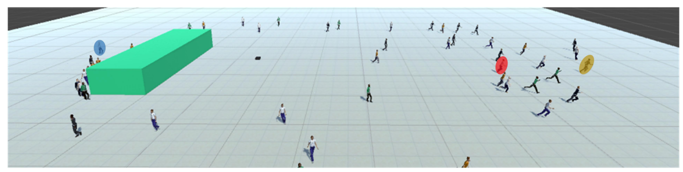

(b) Positions of the individuals at the 80^{th} frame after the hazard occurred

Fig. 4: A virtual simulation scene. The green cube represents the obstacle. The red ellipse is Individual No. 10, the yellow one is No. 35, and the blue one is No. 56. Individual No. 10 can directly perceive the hazard, Individual No. 35 can indirectly perceive the hazard through the emotional contagion, and Individual No. 56 will not be affected by the hazard directly or indirectly.

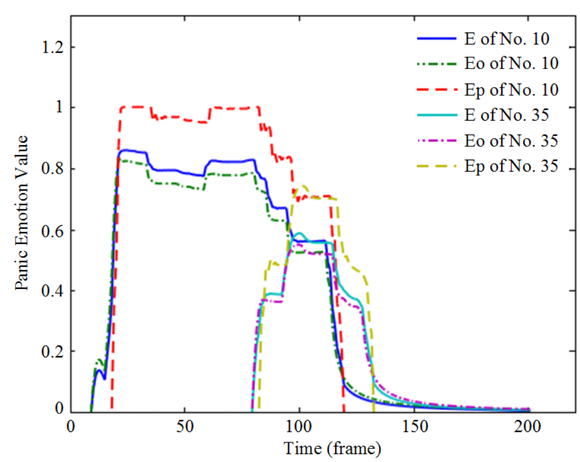

Fig. 5: Panic emotion values of Individuals No. 10 and No. 35. E_p is larger than E_o. The panic emotion value of Individual No. 10 is larger than that of Individual No. 35. The duration of the panic emotion in Individual No. 10 is also longer than that in Individual No. 35.

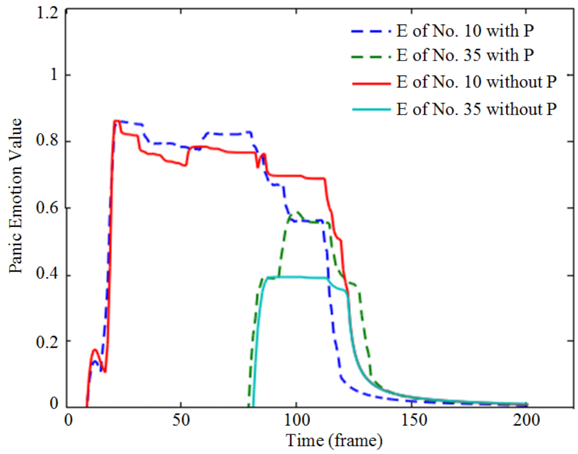

Fig. 6: Panic emotions of Individuals No. 10 and No. 35 with and without considering the physical strength consumption. The panic emotion value of individuals whose physical strength consumption is considered is higher than that of individuals whose physical strength consumption is not considered.

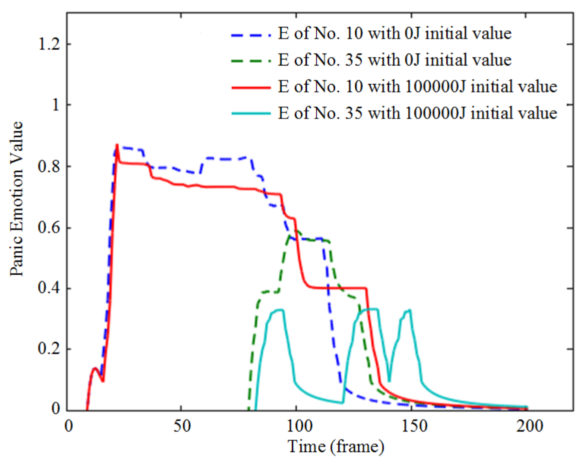

Fig. 7: Panic emotions of individuals with different initial values of physical strength consumption. The panic emotion of the individual with $100{,}000J$ initial value of physical strength consumption is less than the panic emotion of the individual with $0J$ initial value of physical strength consumption. Individual No. 35 can perceive the hazard indirectly through the emotional contagion. The individuals around him have a large influence on his panic emotion. Therefore, the solid blue curve (for $100{,}000J$ initial value) behaves abnormally, as when it exhibits several valleys.

4.1 Relationship evaluation among these three factors

To validate our model, we analyze the panic emotion and moving speed of different individuals with and without considering an individual's physical strength consumption in a virtual crowd scene (shown in Figure 4). Then we analyze the impact of different initial values of physical strength consumption on the panic emotion and speed.

Three individuals in this scene, No. 10, No. 35, and No. 56, are taken as examples. The emotional changes of Individuals No. 10 and No. 35 in the above scene are presented in Figure 5. Compared with Individual No. 35, Individual No. 10 can perceive the hazard directly and is closer to the hazard, so he is more panicked than Individual No. 35.

The panic emotions of different individuals with and without considering the physical strength consumption are shown in Figure 6. As mentioned, physical strength consumption affects emotional experience. Therefore, without considering the physical strength consumption, the emotional experience becomes zero and the final panic emotion does not accumulate this component. Thus, panic emotion values considering physical strength consumption are higher.

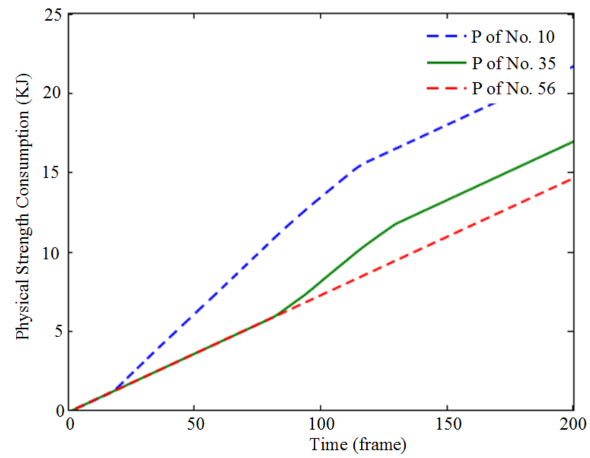

Fig. 8: Physical strength consumption of individuals. Individual No. 10 is more frightened than the other two and his moving speed is faster, so he consumes more physical strength than the other two. Moreover, the slope of his physical strength consumption is also larger than that of the other individuals. Since Individual No. 56 is not panicked, the slope of his physical strength consumption does not change.

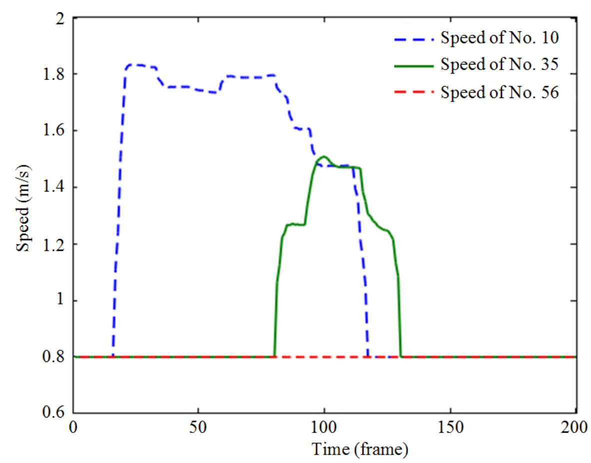

Fig. 9: The moving speeds of different individuals. Individual No. 56 is not panicked. Thus, his moving speed does not change. The remaining two individuals start to move faster when they become panicked. Since Individual No. 10 is more panicked than Individual No. 35, he moves faster.

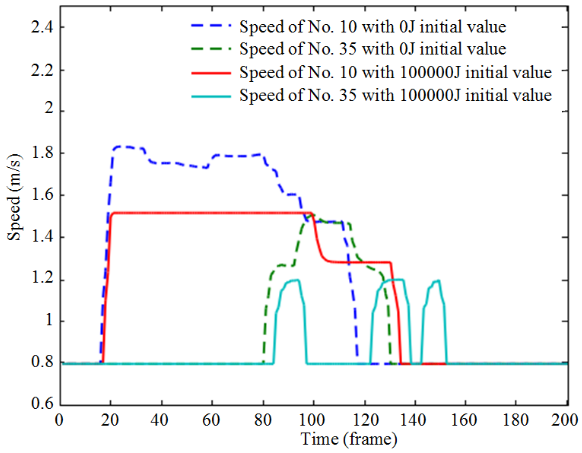

Fig. 10: The speeds of individuals with different initial values of physical strength consumption. The individual with $0J$ initial value of physical strength consumption moves faster than the individual with 100,000J initial value of physical strength consumption. The more panicked an individual is, the faster his moving speed is. Therefore, the solid blue curve (for 100,000J initial value) behaves abnormally, similar to the panic emotion of Individual No. 35 in Figure 7.

The panic emotions of individuals with different initial values of physical strength consumption are presented in Figure 7. If an individual has consumed too much physical strength (initial value of physical strength consumption is 100,000J), the rest of his physical strength will be reduced. Thus, the individual moves slower than before, and physical strength consumption per unit of time for this individual is reduced. When his heart rate drops, according to the James-Lange theory, the emotional experience is reduced. Therefore, the panic emotion of an individual with 100,000J initial value of physical strength consumption is less than the panic emotion of the individual with $0J$ initial value of physical strength consumption.

As shown in Figure 8, the physical strength consumptions of all three individuals change over time. Before the hazard occurs, all the individuals move at the same speed and the speeds of their physical strength consumption are the same. However, when individuals become panicked, the speeds of their physical strength consumption increase significantly. The more panicked the individual is, the more physical strength consumption there is.

The moving speeds of all three individuals with the same initial values of physical strength consumption are presented in Figure 9. The moving speeds with different initial values of physical strength consumption are presented in Figure 10. Both panic emotion and physical strength consumption affect the moving speeds of individuals. The more panicked an individual is, the faster his/her moving speed is. The less physical strength consumption an individual has experienced, the faster his/her moving speed is. Panic emotion affects individuals' moving directions by driving them to run away from the hazard. When individuals are far from the hazard and arrive in a safe place, they are not panicked, and their moving speed is restored to a normal level.

4.2 Comparisons

To validate our approach, we compare the simulation results obtained by different methods with real-world crowd evacuation videos. The trend in the simulation results obtained by our CubeP model is that they are more similar to real-world videos than other approaches.

Comparisons between real scenes and the corresponding simulation results are presented in Figure 11. We take two different real-world scenarios (chosen from the public UMN dataset [61]) as examples, and detailed results can be seen in the supplementary video. The CubeP model is compared with the Durupinar model [11] and the Neto model [36]. We annotate the trajectories of all the individuals in the real-world video using the video annotation tool in [62] and assign initial movement states to the CubeP, Neto, and Durupinar models. Therefore, we can predict the trajectories of these individuals and compare them with the actual ones.

In the Grass scenario, Individual No. 1 moves faster than Individual No. 2, and Individual No. 1 moves closer to Individual No. 2 (Figure 11a). The simulation result obtained by the CubeP model in the Grass scenario is more realistic than that obtained by the Durupinar and Neto models. The reason is that the speed is influenced by physical strength consumption in the CubeP model. If an individual has consumed more physical strength than other individuals, his moving speed decreases and other individuals move faster than he does. Thus, simulating the situation is easier when one individual gets closer to another individual.

TABLE 3: Entropy metric for different simulation algorithms on different scenarios. A lower value of entropy metric implies improved similarity with respect to the real-world crowd videos.

Scenario	CubeP	Durupinar	Neto	SFM
Grass	3.3868	3.4290	3.4097	4.2955
Room	5.3939	5.4632	5.4933	6.1767

In the Room scenario, some individuals are marked with red circles in the simulation results obtained by the Durupinar and Neto models (Figures 11g and 11h). The moving directions and moving speeds of these individuals are almost the same. The collectiveness of the trajectories by the Durupinar and Neto models is much higher than that of the real scene. The simulation result by the CubeP model conforms to the real-world video. The is because the emotion mechanism of the CubeP model changes the moving directions of individuals and drives them to move away from the hazard. Meanwhile, the physical strength consumption influences the individual's speed.

We use the entropy metric [63] to evaluate the trajectories of different simulation algorithms on different scenarios (see Table 3). The social force model is denoted as SFM.

For each scenario, a user study is performed. There are 39 participants (51.28% female, 66.67% in the age group of 20-30) in this study and participants are asked to compare the movement states in the original video clips with the movement states in the crowd simulation results (Figure

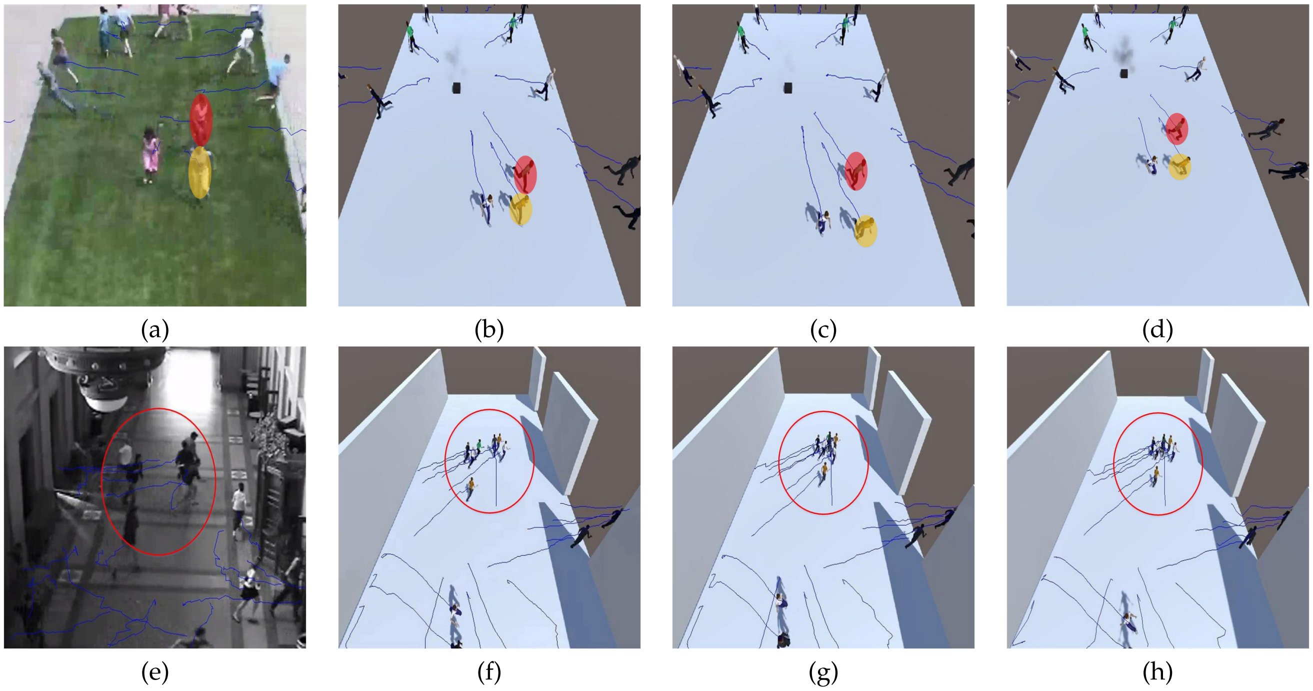

Fig. 11: Comparisons between real scenes and simulation results by different models: (a) and (e) are real-world videos, (b) and (f) are simulated by the CubeP model, (c) and (g) are simulated by the Durupinar model, (d) and (h) are simulated by the Neto model. Each row represents one scene. (a) The red ellipse is Individual No. 1 and the yellow one is Individual No. 2. Individual No. 1 gets closer to Individual No. 2. We present the line charts to show the distance between Individual No. 1 and Individual No. 2 at different time steps (Figure 12a). (b) As the speed is influenced by physical strength consumption, simulating the situation where Individual No. 1 gets closer to Individual No. 2 is easier using the CubeP model. In (g) and (h), the simulation trajectories of different individuals in the red circle by the Durupinar and Neto model are similar and individuals easily get together, which is different from the real-world video. We provide the line charts to show the collectiveness (the collectiveness indicates the degree of individuals in the whole scene acting as a unit in collective motion [59], [60]) of simulation results and the real-world video at different time steps (Figure 12b). The collectiveness of simulations by the Durupinar and Neto models is much higher than that of the real-world video.

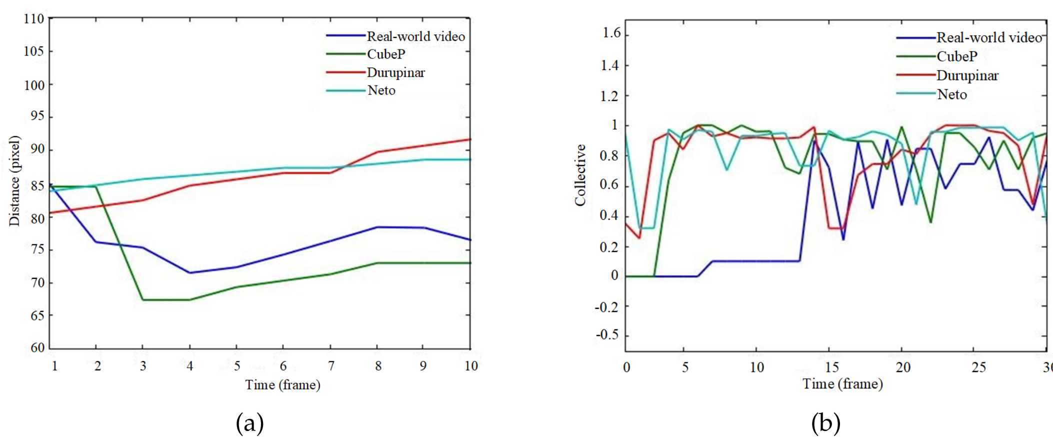

Fig. 12: Quantitative comparisons between real scenes and simulation results by different models: (a) Distance between Individual No. 1 and Individual No. 2 in the Grass scenario of Figure 11. (b) Collectiveness in the Room scenario of Figure 11.

13). Table 3 and Figure 13 show that the simulated moving trends of the CubeP model are closer to those in the real-world videos than other models. A rational approach is to combine physical strength consumption and panic emotion to determine the movement of each individual.

We take two real scenarios as examples to verify our proposed crowd simulation method. Crowd simulation by the CubeP model of the scene after the mobile phone explosion on the subway in the Shanghai Metro Line 8 is presented in Figures 14a and 14b. Crowd simulation of the shooting at the British Parliament building on March 22, 2017 by the CubeP model is presented in Figures 14c and 14d. We

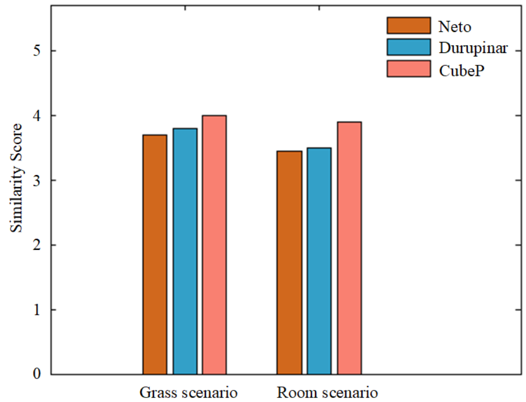

Fig. 13: Comparison of similarity scores for movement states (higher values indicate greater similarity). We compare the movement states in the original videos with those in crowd simulation results achieved by different algorithms.

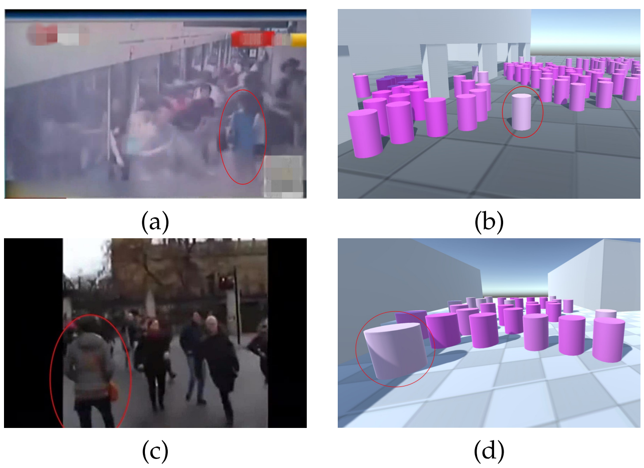

Fig. 14: Comparisons between real-world videos and simulation results by our approach. (a) The mobile phone explosion incident on the subway in the Shanghai Metro Line 8; (c) The shooting incident at the British Parliament building on March 22, 2017; (b,d) our corresponding simulation results with the CubeP model. At first, the individuals in the red circle aren't panicked. Because of emotional contagion, they are then influenced by the panicked crowd around them, become panicked, and run away from the hazards.

show the spread of the panic emotion in both scenarios. The color of the cylinders represents the emotional intensity of the individuals. From our simulation results and Figure 15, we can see that both the overall moving trend and the process of emotional contagion are similar to those found in the recorded real-world crowd video clips.

In the Virtual scenario, we compare our simulation result with those of the Durupinar [11], Neto [36], and CubeP with Neto models. In both the CubeP and Durupinar models, each factor of personality satisfies normal distribution $N(0, 0.25)$ [11]. In the Neto and CubeP with Neto models, $\epsilon = 0.5$, $\delta = 0.5$, $\eta = 0.5$, and $\beta = 1$ [36]. In Figure 16a (the simulation result by the Durupinar model), the speeds of individuals are variable and their locations are

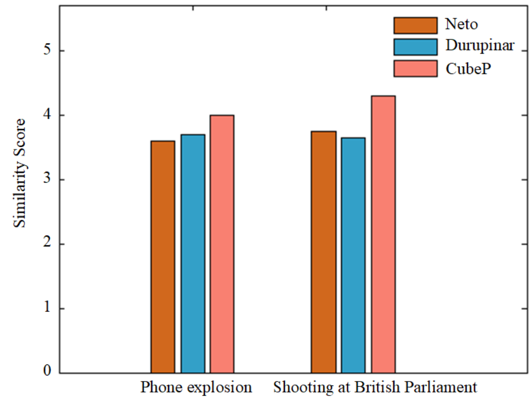

Fig. 15: Comparison of similarity scores for movement states and the process of emotional contagion (higher values indicate greater similarity). A user study is performed and participants are asked to compare the movement states and processes of emotional contagion in the original videos with those in crowd simulation results achieved by different algorithms.

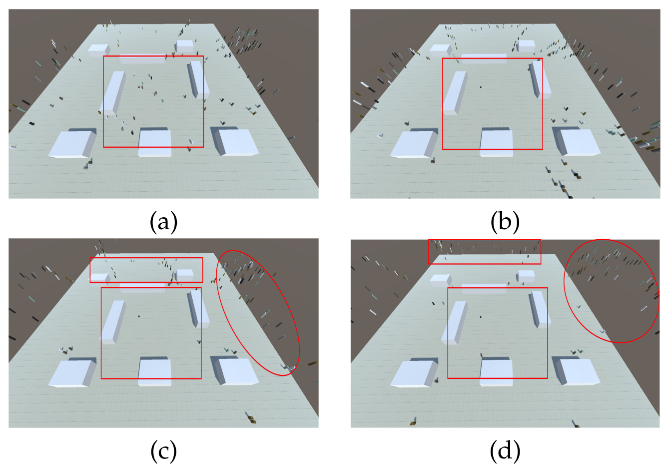

Fig. 16: Crowd simulation results by different models in the Virtual scenario at the $1000th$ frame: (a) Durupinar model, (b) Neto model, (c) CubeP with neto model, and (d) CubeP model.

scattered. Because of different thresholds and personality mechanisms, the Durupinar model can simulate heterogeneous crowd behavior. However, there are too many individuals who are not affected by the panicked crowd and this result is unreasonable. In Figure 16b, individuals move much slower than the individuals in the simulation results by other models. The reason is that the emotion calculated by the Neto model is much smaller. Moreover, the individual movement is too regular, which is unsuitable for emergency situations. In Figure 16c (simulation result by the CubeP with Neto model) and Figure 16d (simulation result by the CubeP model), most of the individuals are affected by the hazard and run away from it. Because of physical strength consumption and personality factors, the speeds of individuals in the simulation result by the CubeP model are more variable than those shown in the CubeP with Neto model. Therefore, the simulation result by the CubeP model is more suitable for emergency situations than other models.

4.3 Application of the CubeP model in various virtual scenarios

(a)

(b)

Fig. 17: Crowd simulation results at a subway station: (a) the higher level of the subway station, (b) the lower level of the subway station. After the hazard occurs, the emotional contagion in our model begins to work. Although the direct impact of the hazard is limited, the hazardous area grows through emotional contagion among individuals and the number of individuals who run away from the hazard increases.

The CubeP model can be applied in different virtual scenarios. Subway station and crosswalk are crowded and the probability of hazard occurrence in these scenarios is very high. We simulate a hazard occurring in these scenarios and three examples are shown. Figure 17(a) shows crowd simulation at the higher level of the subway station. Figure 17(b) shows crowd simulation at the lower level of the subway station. Figure 18 shows crowd simulation at a crosswalk. We show each step of the process: hazard occurring, individuals running away from the hazard, emotional contagion, and the attenuation of moving speed. More details can be seen in the supplementary video. Our simulation results provide information about decision-making to deal with emergency situations.

The heat maps of panic emotion in the Virtual scene are presented in Figure 19. Although the direct impact of the hazard is limited, the panic area grows through the emotional contagion mechanism in the CubeP model. When individuals are far from the hazard, panic emotion attenuates. As accidents may happen in public places randomly, we can take preventive action in advance and reduce loss by accurately predicting the panic area.

Fig. 18: Crowd simulation result at a crosswalk. At the lower left corner, a car explodes. Then individuals run away from the hazard.

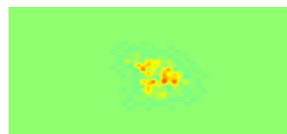

(a)

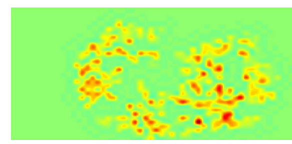

(b)

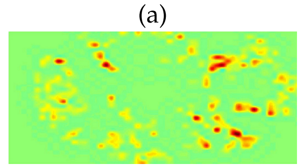

(c)

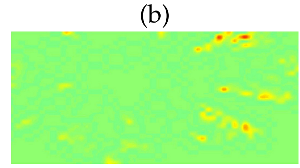

(d)

Fig. 19: Panic emotion heat maps of the Virtual scene: (a) heat map at the 13^{th} frame, (b) heat map at the 29^{th} frame, (c) heat map at the 57^{th} frame, (d) heat map at the 120^{th} frame. The red area is more panicked than the green area in the heat map. The deeper the color is, the more panicked the area is.

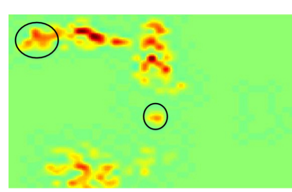

(a)

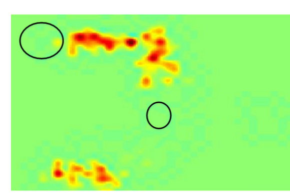

(b)

Fig. 20: The heat maps of panic emotion at the 185^{th} frame of the crosswalk scenario: (a) heat map of the CubeP model crowd simulation result, and (b) heat map of the Durupinar model crowd simulation result. The red area is more panicked than the green area in the heat map. The deeper the color is, the more panicked the area is. We highlight the same area of the two simulation results. The individuals in the CubeP model simulation result are more panicked than the individuals in the Durupinar model simulation results.

The heat maps of panic emotion in crowd simulations in the crosswalk scenario by the CubeP and Durupinar models are presented in Figure 20. The individuals in the CubeP model simulation results are more panicked than those in the Durupinar model simulation results. The intensity of the panic emotion calculated by the Durupinar model is lower than that calculated by the CubeP model. The reason is that the CubeP model considers not only emotional contagion among individuals, but also the impact of physical strength consumption on panic emotion. The CubeP model represents a comprehensive description of individual panic emotion and is more conducive to the spread of panic emotion than the Durupinar model. Therefore, the simulation results by the CubeP model are more reasonable for emergency situations.

5 Conclusion and Limitations

In contrast to traditional individual behavior models that consider only physiological, psychological, or physical aspects, we propose a comprehensive model for emergency crowd simulation by combing these three aspects. We not only present a physical strength consumption calculation and a panic emotion calculation, but also delineate the relationship between them. We comprehensively analyze physical strength consumption and panic emotion. Finally, both physical strength consumption and panic emotion determine the movement of each individual. In addition, individual movements affect individual physical strength consumption and panic emotion by emphasizing the interaction of individual physiological, psychological, and physical factors. Our proposed model is verified by simulations, and it is compared with real-world videos and previous approaches. Results have shown that our proposed model can reliably generate realistic group behavior. It can also predict the changes of physical strength consumption and panic emotion of a crowd in an emergency situation.

However, our model has several limitations. Although the CubeP model can generate realistic crowd movement, the panic emotion and physical strength consumption of the crowd in an emergency scene cannot be obtained directly. Our model can only infer them during the simulation. Thus, the initial state of our model is difficult to determine and it is usually time consuming to do so. In the future, we plan to use the latest wearable equipment to collect these data and provide a new method that can quickly and accurately determine the initial state. Furthermore, at present, our model mainly focuses on emergency scenarios. In future work, we want to extend the CubeP model to a variety of general situations.

References

[1] M. Xu, H. Jiang, X. Jin, and Z. Deng, "Crowd simulation and its applications: Recent advances," *Journal of Computer Science and Technology*, vol. 29, no. 5, pp. 799–811, 2014.

[2] Á. Gómez, L. López-Rodríguez, H. Sheikh, J. Ginges, L. Wilson, H. Waziri, A. Vázquez, R. Davis, and S. Atran, "The devoted actor's will to fight and the spiritual dimension of human conflict," *Nature Human Behaviour*, vol. 1, pp. 673–679, 2017.

[3] M. Xu, Y. Wu, P. Lv, H. Jiang, M. Luo, and Y. Ye, "miSFM: On combination of mutual information and social force model towards simulating crowd evacuation," *Neurocomputing*, vol. 168, pp. 529–537, 2015.

[4] J. Chun, H. Lee, Y. S. Park, W. Park, J. Park, S. H. Han, S. Choi, and G. J. Kim, "Real-time classification of fear/panic emotion based on physiological signals." in *Proc. The Eighth Pan-Pacific Conference on Occupational Ergonomics*, 2007, pp. 1–9.

[5] J. W. Kalat, *Biological Psychology (10th ed.)*. Cengage Learning, 2007.

[6] Y. Li, M. Christie, O. Siret, and R. Kulpa, "Cloning crowd motions," in *Proc. ACM SIGGRAPH/Eurographics Symp. Comput. Animation*, 2012, pp. 201–210.

[7] J. Koo, B. I. Kim, and Y. S. Kim, "Estimating the effects of mental disorientation and physical fatigue in a semi-panic evacuation," *Expert Systems with Applications*, vol. 41, no. 5, pp. 2379–2390, 2014.

[8] J. M. Frederic P. Miller, Agnes F. Vandome, *Physical Strength*. Alphascript Publishing, 2011.

[9] W. R. Leonard, "Measuring human energy expenditure: What have we learned from the flex-heart rate method?" *American Journal of Human Biology*, vol. 15, no. 4, pp. 479–489, 2003.

[10] D. M. Buchner, E. B. Larson, E. H. Wagner, T. D. Koepsell, and B. J. De Lateur, "Evidence for a non-linear relationship between leg strength and gait speed," *Age and Ageing*, vol. 25, no. 5, pp. 386–391, 1996.

[11] F. Durupınar, U. Güdükbay, A. Aman, and N. I. Badler, "Psychological parameters for crowd simulation: From audiences to mobs," *IEEE Transactions on Visualization and Computer Graphics*, vol. 22, no. 9, pp. 2145–2159, 2016.

[12] D. Helbing, I. Farkas, and T. Vicsek, "Simulating dynamical features of escape panic," *Nature*, vol. 407, no. 6803, pp. 487–490, 2000.

[13] L. Zheng, D. Qin, Y. Cheng, L. Wang, and L. Li, "Simulating heterogeneous crowds from a physiological perspective," *Neurocomputing*, vol. 172, no. C, pp. 180–188, 2012.

[14] S. Kim, S. J. Guy, D. Manocha, and M. C. Lin, "Interactive simulation of dynamic crowd behaviors using general adaptation syndrome theory," in *Proc. Symp. Interactive 3D Graphics and Games*, 2012, pp. 55–62.

[15] S. J. Guy, J. Chhugani, S. Curtis, P. Dubey, M. Lin, and D. Manocha, "PLEdestrians: a least-effort approach to crowd simulation," in *Proc. ACM SIGGRAPH/Eurographics Symp. Comput. Animation*, 2010, pp. 119–128.

[16] S. Kim, A. Bera, A. Best, R. Chabra, and D. Manocha, "Interactive and adaptive data-driven crowd simulation," in *Proc. IEEE Virtual Reality Conf.*, Mar. 2016, pp. 29–38.

[17] H. L. Kang, M. G. Choi, Q. Hong, and J. Lee, "Group behavior from video:a data-driven approach to crowd simulation," in *Proc. ACM SIGGRAPH/Eurographics Symp. Comput. Animation*, 2007, pp. 109–118.

[18] I. Karamouzas, N. Sohre, R. Narain, and S. J. Guy, "Implicit crowds: optimization integrator for robust crowd simulation," *ACM Transactions on Graphics*, vol. 36, no. 4, pp. 1–13, 2017.

[19] S. Yi, H. Li, and X. Wang, "Pedestrian behavior modeling from stationary crowds with applications to intelligent surveillance," *IEEE Transactions on Image Processing*, vol. 25, no. 9, pp. 4354–4368, 2016.

[20] T. Feng, L. F. Yu, S. K. Yeung, K. K. Yin, and K. Zhou, "Crowd-driven mid-scale layout design," *ACM Transactions on Graphics*, vol. 35, no. 4, pp. 132–145, 2016.

[21] N. M. Joseph, N. M. Joseph, N. M. Joseph, N. M. Joseph, N. M. Joseph, and N. M. Joseph, "Zootopia crowd pipeline," in *Proc. ACM SIGGRAPH*, 2016, pp. 59:1–59:2.

[22] V. J. Cassol, E. S. Testa, C. R. Jung, M. Usman, P. Faloutsos, G. Berseth, M. Kapadia, N. I. Badler, and S. R. Musse, "Evaluating and optimizing evacuation plans for crowd egress," *IEEE Computer Graphics & Applications*, vol. 37, no. 4, pp. 60–71, 2017.

[23] M. Zucker, J. Kuffner, and M. Branicky, "Multipartite RRTs for rapid replanning in dynamic environments," in *Proc. IEEE Conf. Robotics and Automation*, 2007, pp. 1603–1609.

[24] B. Kluge and E. Prassler, "Reflective navigation: Individual behaviors and group behaviors," in *Proc. IEEE Conf. Robotics and Automation*, 2004, pp. 4172–4177.

[25] H. Wang, J. Ondřej, and C. OSullivan, "Trending paths: A new semantic-level metric for comparing simulated and real crowd data," *IEEE Transactions on Visualization and Computer Graphics*, vol. 23, no. 5, pp. 1454–1464, 2017.

[26] T. Weiss, A. Litteneker, C. Jiang, and D. Terzopoulos, "Position-based multi-agent dynamics for real-time crowd simulation," in *Proc. ACM SIGGRAPH/Eurographics Symp. Comput. Animation*, 2017, pp. 27:1–27:2.

[27] L. He, J. Pan, S. Narang, and D. Manocha, "Dynamic group behaviors for interactive crowd simulation," in *Proc. ACM SIGGRAPH/Eurographics Symp. Comput. Animation*, 2016, pp. 139–147.
[28] M. Xu, Y. Wu, Y. Ye, I. Farkas, H. Jiang, and Z. Deng, "Collective crowd formation transform with mutual informationcbased runtime feedback," *Computer Graphics Forum*, vol. 34, no. 1, pp. 60–73, 2015.
[29] F. Belkhouche, "Reactive path planning in a dynamic environment," *IEEE Transactions on Robotics*, vol. 25, no. 4, pp. 902–911, 2009.
[30] S. Patil, J. Van Den Berg, S. Curtis, M. C. Lin, and D. Manocha, "Directing crowd simulations using navigation fields," *IEEE Transactions on Visualization and Computer Graphics*, vol. 17, no. 2, pp. 244–254, 2011.
[31] R. Kulpa, A. Olivierxs, J. Ondřej, and J. Pettré, "Imperceptible relaxation of collision avoidance constraints in virtual crowds," *ACM Transactions on Graphics*, vol. 30, no. 6, pp. 138:1–138:10, 2011.
[32] R. Gayle, A. Sud, E. Andersen, S. J. Guy, M. C. Lin, and D. Manocha, "Interactive navigation of heterogeneous agents using adaptive roadmaps," *IEEE Transactions on Visualization and Computer Graphics*, vol. 15, no. 1, pp. 34–48, 2009.
[33] A. Sud, E. Andersen, S. Curtis, M. C. Lin, and D. Manocha, "Real-time path planning in dynamic virtual environments using multiagent navigation graphs," *IEEE Transactions on Visualization and Computer Graphics*, vol. 14, no. 3, pp. 526–538, 2008.
[34] A. Golas, R. Narain, S. Curtis, and M. C. Lin, "Hybrid long-range collision avoidance for crowd simulation," *IEEE Transactions on Visualization and Computer Graphics*, vol. 20, no. 7, pp. 1022–1034, 2014.
[35] M. Xu, Z. Pan, M. Zhang, P. Lv, P. Zhu, Y. Ye, and W. Song, "Character behavior planning and visual simulation in virtual 3d space," *IEEE Multimedia*, vol. 20, no. 1, pp. 49–59, 2013.
[36] A. B. F. Neto, C. Pelachaud, and S. R. Musse, "Giving emotional contagion ability to virtual agents in crowds," in *Proc. Intelligent Virtual Agents*, 2017, pp. 63–72.
[37] H. Jiang, Z. Deng, M. Xu, X. He, T. Mao, and Z. Wang, "An emotion evolution based model for collective behavior simulation," in *Proc. Symp. Interactive 3D Graphics and Games*, 2018, pp. 10:1–10:6.
[38] A. Ortony, G. L. Clore, and A. Collins, "The cognitive structure of emotions." *Contemporary Sociology*, vol. 18, no. 6, pp. 2147–2153, 1988.
[39] L. Berkowitz, "On the formation and regulation of anger and aggression: A cognitive-neoassociationistic analysis." *American Psychologist*, vol. 45, no. 4, p. 494, 1990.
[40] W. O. Kermack and A. G. McKendrick, "Contributions to the mathematical theory of epidemics. III. further studies of the problem of endemicity," *Proc. the Royal Society of London. Series A*, vol. 141, no. 843, pp. 94–122, 1933.
[41] L. Zhao, H. Cui, X. Qiu, X. Wang, and J. Wang, "SIR rumor spreading model in the new media age," *Physica A: Statistical Mechanics and its Applications*, vol. 392, no. 4, pp. 995–1003, 2013.
[42] S. H. White, A. M. Del Rey, and G. R. Sánchez, "Modeling epidemics using cellular automata," *Applied Mathematics and Computation*, vol. 186, no. 1, pp. 193–202, 2007.
[43] F. Durupinar, N. Pelechano, J. Allbeck, U. Gudukbay, and N. I. Badler, "How the ocean personality model affects the perception of crowds," *IEEE Computer Graphics and Applications*, vol. 31, no. 3, pp. 22–31, 2011.
[44] J. H. Wang, S. M. Lo, J. H. Sun, Q. S. Wang, and H. L. Mu, "Qualitative simulation of the panic spread in large-scale evacuation," *Simulation*, vol. 88, no. 12, pp. 1465–1474, 2012.
[45] L. Fu, W. Song, W. Lv, and S. Lo, "Simulation of emotional contagion using modified SIR model: a cellular automaton approach," *Physica A: Statistical Mechanics and its Applications*, vol. 405, pp. 380–391, 2014.
[46] T. Bosse, R. Duell, Z. A. Memon, J. Treur, and C. N. V. D. Wal, "A multi-agent model for mutual absorption of emotions," *in Proc. 23th EuropeanConf. Mod. and Sim.*, 2009.
[47] J. Tsai, E. Bowring, S. Marsella, and M. Tambe, "Empirical evaluation of computational fear contagion models in crowd dispersions," *Autonomous Agents and Multi-agent Systems*, vol. 27, no. 2, pp. 200–217, 2013.
[48] J. Bruneau, A.-H. Olivier, and J. Pettre, "Going through, going around: A study on individual avoidance of groups," *IEEE Transactions on Visualization and Computer Graphics*, vol. 21, no. 4, pp. 520–528, 2015.
[49] L. Keytel, J. Goedecke, T. Noakes, H. Hiiloskorpi, R. Laukkanen, L. van der Merwe, and E. Lambert, "Prediction of energy expenditure from heart rate monitoring during submaximal exercise," *Journal of Sports Sciences*, vol. 23, no. 3, pp. 289–297, 2005.
[50] S. J. Guy, J. Chhugani, C. Kim, N. Satish, M. Lin, D. Manocha, and P. Dubey, "Clearpath: highly parallel collision avoidance for multi-agent simulation," in *Proc. ACM SIGGRAPH/Eurographics Symp. Comput. Animation*, 2009, pp. 177–187.
[51] S. J. Ulijaszek, "Human energetics in biological anthropology," *American Journal of Human Biology*, vol. 8, no. 5, pp. 682–683, 2010.
[52] J. Nilsson and A. Thorstensson, "Ground reaction forces at different speeds of human walking and running," *Acta Physiologica*, vol. 136, no. 2, pp. 217–227, 1989.
[53] R. Cross, "Standing, walking, running, and jumping on a force plate," *American Journal of Physics*, vol. 67, no. 4, pp. 304–309, 1999.
[54] J. M. Burnfield, Y. J. Tsai, and C. M. Powers, "Comparison of utilized coefficient of friction during different walking tasks in persons with and without a disability," *Gait & Posture*, vol. 22, no. 1, pp. 82–88, 2005.
[55] J. Tsai, E. Bowring, S. Marsella, and M. Tambe, "Empirical evaluation of computational emotional contagion models," in *Proc. Intelligent Virtual Agents*, 2011, pp. 384–397.
[56] A. E. Basak, U. Gudukbay, and F. Durupinar, "Using real life incidents for realistic virtual crowds with data-driven emotion contagion," *Computers & Graphics*, vol. 72, 2018.
[57] D. Wolinski, S. J. Guy, A. H. Olivier, M. Lin, and D. Manocha, "Parameter estimation and comparative evaluation of crowd simulations," *Computer Graphics Forum*, vol. 33, no. 2, pp. 303–312, 2014.
[58] H. M. Petry and O. Desiderato, "Changes in heart rate, muscle activity, and anxiety level following shock threat," *Psychophysiology*, vol. 15, no. 5, pp. 398–402, 1978.
[59] J. Shao, K. Kang, C. L. Chen, and X. Wang, "Deeply learned attributes for crowded scene understanding," in *Proc. IEEE Conf. Comput. Vis. Pattern Recognit*, 2015, pp. 4657–4666.
[60] M. Xu, C. Li, P. Lv, N. Lin, R. Hou, and B. Zhou, "An efficient method of crowd aggregation computation in public areas," *IEEE Transactions on Circuits & Systems for Video Technology*, vol. PP, no. 99, pp. 1–12, 2017.
[61] R. Mehran, A. Oyama, and M. Shah, "Abnormal crowd behavior detection using social force model," in *Proc. IEEE Conf. Comput. Vis. Pattern Recognit*, 2009, pp. 935–942.
[62] C. Vondrick, D. Patterson, and D. Ramanan, "Efficiently scaling up crowdsourced video annotation," *Int. J. Comput. Vision*, vol. 101, no. 1, pp. 184–204, 2013.
[63] S. J. Guy, J. V. D. Berg, W. Liu, R. Lau, M. C. Lin, and D. Manocha, "A statistical similarity measure for aggregate crowd dynamics," *ACM Transactions on Graphics*, vol. 31, no. 6, pp. 1–11, 2012.

Mingliang Xu is a full professor in the School of Information Engineering of Zhengzhou University, China, and currently is the director of CIISR (Center for Interdisciplinary Information Science Research) and the vice General Secretary of ACM SIGAI China. He received his Ph.D. degree in computer science and technology from the State Key Lab of CAD&CG at Zhejiang University, Hangzhou, China. His current research interests include computer graphics, multimedia and artificial intelligence.

Chaochao Li is a Ph.D candidate in the School of Information Engineering of Zhengzhou University, China, and his research interest is computer graphics and computer vision.

Pei Lv is an associate professor in School of Information Engineering, Zhengzhou University, China. His research interests include video analysis and crowd simulation. He received his Ph.D in 2013 from the State Key Lab of CAD&CG, Zhejiang University, China.

Wei Chen is a professor at the State Key Lab of CAD&CG, Zhejiang University. His research interests is on visualization and visual analysis, and has published more than 30 IEEE/ACM Transactions and IEEE VIS papers. He actively served as guest or associate editors of IEEE Transactions on Visualization and Computer Graphics, IEEE Transactions on Intelligent Transportation Systems, and Journal of Visualization. For more information, please refer to http://www.cad.zju.edu.cn/home/chenwei/.

Zhigang Deng is a Full Professor of Computer Science at University of Houston (UH). He is also the Director of Graduate Studies at UH Computer Science Department and the Founding Director of the UH Computer Graphics and Interactive Media (CGIM) Lab. He earned Ph.D. in Computer Science at the Integrated Media System Center (NSF ERC) and Department of Computer Science at the University of Southern California in 2006. He completed B.S. degree in Mathematics from Xiamen University (China), and M.S. in Computer Science from Peking University (China).His interests are in the broad areas of computer graphics, computer animation, human computer interaction, virtual human modeling and animation, and visual computing for biomedical/healthcare informatics. He is the recipient of ACM ICMI Ten Year Technical Impact Award, UH Teaching Excellence Award, Google Faculty Research Award, UHCS Faculty Academic Excellence Award, and NSFC Overseas and Hong Kong/Macau Young Scholars Collaborative Research Award. Besides the CASA 2014 conference general co-chair and SCA 2015 conference general co-chair, He currently serves as an Associate Editor of several journals including Computer Graphics Forum, and Computer Animation and Virtual Worlds Journal.

Bing Zhou is currently a professor at the School of Information Engineering, Zhengzhou University, Henan, China. He received the B.S. and M.S. degrees from Xian Jiao Tong University in 1986 and 1989, respectively,and the Ph.D. degree in Beihang University in 2003, all in computer science. His research interests cover video processing and understanding, surveillance, computer vision, multimedia applications.

Dinesh Manocha is the Paul Chrisman Iribe Chair in Computer Science & Electrical and Computer Engineering at the University of Maryland College Park. He is also the Phi Delta Theta/Matthew Mason Distinguished Professor Emeritus of Computer Science at the University of North Carolina - Chapel Hill. He has won many awards, including Alfred P. Sloan Research Fellow, the NSF Career Award, the ONR Young Investigator Award, and the Hettleman Prize for scholarly achievement. His research interests include multi-agent simulation, virtual environments, physically-based modeling, and robotics. His group has developed a number of packages for multi-agent simulation, crowd simulation, and physics-based simulation that have been used by hundreds of thousands of users and licensed to more than 60 commercial vendors. He has published more than 500 papers and supervised more than 35 PhD dissertations. He is an inventor of 9 patents, several of which have been licensed to industry. His work has been covered by the New York Times, NPR, Boston Globe, Washington Post, ZDNet, as well as DARPA Legacy Press Release. He is a Fellow of AAAI, AAAS, ACM, and IEEE and also received the Distinguished Alumni Award from IIT Delhi. He was a co-founder of Impulsonic, a developer of physics-based audio simulation technologies, which was acquired by Valve Inc. See http://www.cs.umd.edu/~dm